Photonic crystal structures based on submicron particles of polymethyl methacrylate

Photonic crystal structures based on submicron particles of polymethyl methacrylate

I V Nemtsev[1,2,3], O V Shabanova[4], N P Shestakov[2], A A Ivanenko[1,2], A V Cherepakhin[2,3], V Ya Zyryanov[1,2]

[1]Federal Research Center "Krasnoyarsk Science Center of the Siberian Branch of the Russian Academy of Sciences", Akademgorodok street 50, Krasnoyarsk, Russia, 660036
[2]Kirensky Institute of Physics, Federal Research Center "Krasnoyarsk Science Center of the Siberian Branch of the Russian Academy of Sciences", Akademgorodok street 50, bul. 38, Krasnoyarsk, Russia, 660036
[3]Siberian Federal University, Svobodny ave. 79, Krasnoyarsk, Russia, 660041
[4]Special Designing and Technological Bureau "Nauka" Federal Research Center "Krasnoyarsk Scientific Center of the Siberian Branch of the Russian Academy of Sciences", Akademgorodok street 50, Krasnoyarsk, Russia, 660036

Abstract. Morphological parameters, reflection spectra, IR absorption spectra, and glass transition temperatures of submicron-sized spheres of poly(methyl methacrylate) (PMMA) formed in a water-acetone dispersion medium were studied in comparison with similar spheres obtained in distilled water. Dependence of a shrinkage degree of the submicrospheres on the concentration of acetone in water is studied. Features of the formation of periodic structures based on the water-acetone dispersions of PMMA in four different ways are considered. 2D (photonic crystal films) and 3D (artificial and inverse opals) resonance structures were obtained.

1. Introduction

Poly(methyl methacrylate) (PMMA) is a well-known amorphous synthetic polymer. It is also known as an "organic glass" due to high optical transparency. Colloidal dispersions of PMMA in various media are promising and attractive materials for a practical application in biomedical, sensor, electrochemical, and electrically conductive devices, optical polymer materials, analytical separators, solar cells, cell technologies, for nanotechnology applications and others [1]. As for the biomedical application, PMMA is seen as the most promising polymer because of its nontoxicity, less cost, minimal inflammatory reactions with tissues, as well as easy processability. Among the applications, drug delivery, implant material, biological labeling, therapy, bio-detection, bio-imaging should be noted [2–4]. Besides, PMMA is one of the most commonly used microfluidic polymers [5]. The possible optical applications include temperature sensors and three-dimensional displays, low-loss transmission, improved absorption, and multifunctional and multi-reactive luminescence [6–8].

The organic glass can also be used for the manufacture of monodispersed micro- and nanospheres [9]. Such beads can form perfectly ordered 2D and 3D mesoporous structures (photonic crystal films,

artificial opals) [10]. It should be noted that there are works devoted to the use of optical devices based on photonic crystals (PhCs) [11]. The examples of the polymer-based PhCs are given in [12,13].

A particular case of PhC is inverse opal (IO) [14,15]. Macroporous structures of IO have promising applications in gas analysis, photo-catalysis, and even in the treatment of cancer cells. Currently, polymer templates are usually used for the manufacture of IO. An essential part of the production of IOs is the manufacture of the PMMA template [16], which has sufficient strength. Therefore, the hardening of the PMMA opal by sintering is required. Thus, an understanding of the chemical and thermal properties, such as the annealing temperature, the tacticity of the polymer, the length of the polymer chain, plays a crucial role in strengthening the PMMA matrix by lightly melting polymer particles.

The properties of the classical PMMA submicrospheres (a classical approach to the synthesis of PMMA particles is an emulsion emulsifier-free polymerization) are well studied. However, using a more complex dispersion medium, it is possible to modify the polymerization procedure [17,18] and obtain microparticles with various properties [19]. The purpose of this study is to develop a methodology for manufacturing spherical polymer submicroparticles from PMMA in an aqueous-acetone dispersion medium to obtain a stable photonic crystal opal template.

2. Materials and methods

2.1. Instrumentation

Measurements of attenuated total reflection (ATR) were carried out in situ on an FTIR spectrometer FT-801 (Simex, Novosibirsk, Russia) to control the synthesis process. To ensure electrical conductivity before microscopy, a K575XD magnetron sputter coating device (Emitech, London, UK) was used to coat the PMMA surface with a thin platinum film. Morphological features of the samples were studied using an FE-SEM S-5500 ultra-high resolution scanning electron microscope (Hitachi, Tokyo, Japan) at an accelerating voltage of 3 kV. The SU3500 scanning electron microscope (Hitachi, Tokyo, Japan) was used to visualize large areas of PMMA opal films and three-dimensional PhC structures: opals and inverse opals. Samples were dried in a laboratory furnace with a digital thermometer SIBLAB 30L 350°C (DION, Novosibirsk, Russia). The Vertex 70 FTIR spectrometer (Bruker, Berlin, Germany) was used to obtain vibrational IR spectra. The Vertex 80v FTIR spectrometer with A513 attachment was used to obtain reflection spectra with a variable angle. To study the glass transition temperature, calorimetric studies were carried out using a Phoenix 204 F-1 premium differential scanning calorimeter (NETZSCH, Berlin, Germany).

2.2. Synthesis of poly (methyl methacrylate) submicrospheres

The PMMA submicroparticles with a polydispersity of less than 5 % [20,21] were fabricated in distilled water (submicrospheres B) to compare them with the same obtained in an aqueous-acetone dispersion medium (submicrospheres A). By the method of a chain radical polymerization of methyl methacrylate [22], nine batches of the high-quality PMMA submicrospheres with the very narrow polydispersity were synthesized. The average diameters in batches were between 237 and 447 nm (Table 1). Every 5 minutes, the FTIR spectra of the emulsion were recorded in situ using FT-801 to control at least two polymerization peculiarities. Firstly, it is necessary to determine whether the polymerization process is completed (a sharp increase in temperature at the deep stages of the reaction, since a hard gel effect is typical for the MMA polymerization). Secondly, make sure that no monomer remains in the dispersion.

2.3. Self-assembly of opal-like colloidal structures

Periodic colloidal structures based on monodisperse spherical particles of PMMA were made by four different methods:

I. Gravity vertical deposition. The dispersion was deposited in hermetically sealed bottles at room temperature for several months.

II. Obtaining PhC by a hybrid method. The hot dispersion (immediately after preparation) was poured with a thin layer (7 mm) into flat substrates coated with polytetrafluoroethylene and dried for 2 weeks.
III. Meniscus. Hot dispersions were poured into plastic cups (100-120 ml) and dried for several weeks until the liquid completely evaporated. Particles were stacked vertically on the walls of the cup, forming a regular PhC structure 2-3 mm thick
IV. Horizontal evaporation. Coverslips were lowered into undiluted dispersions and laid out in Petri dishes horizontally for drying at room temperature.

Table 1. Parametric table of some samples of the submicrospheres A and B

Sample number	MMA volume, ml	Water volume, ml	Acetone volume, ml	Synthesis temperature, °C	The average particle diameter before shrinkage, nm	The degree of shrinkage, %	The average initial dynamic viscosity of the dispersion medium, μPa·s
1	100	620	0	75	303	18	852
2	100	590	30	75	330	9	818
3	100	550	70	72.7	358	7	773

The purpose of this stage was not to obtain highly ordered opals with a single crystal structure, as in [23–25], but to study various ordering defects using different methods of self-assembly.

To estimate the size of the individual PMMA beads they were scanned at a small magnification at an accelerating voltage of 3 kV and beam current of 10 μA, with a maximum resolution (2560x1920 pixels) and the slowest speed. This operation mode minimizes noise and damaging of the polymer particles, but at the same time provides the ability to use digital processing of SEM images using PC. Then the program for editing raster images GIMP (GNU Image Manipulation Program) was employed to estimate the size of submicrospheres. The method is described in more detail in [22].

3. Results and discussion

A study of the PMMA templates prepared in various ways was carried out. Fig. 1 shows the shrinkage of sample 3 (aqueous-acetone) and sample 1 (distilled water) for comparison. Here we see the shrinkage rate of 18% of submicrospheres B and only 7% of the submicrospheres A.

Due to less shrinkage of PMMA beads (admixture of acetone), the PhC opal films have a smaller width of cracks in contrast to the opal films obtained from distilled water (Figs. 2a, 2b).

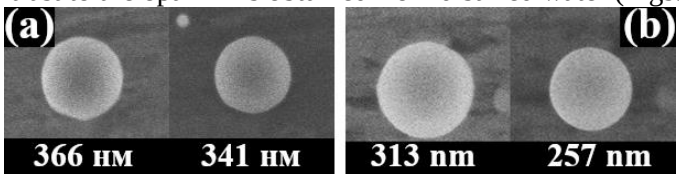

Figure 1. Electron micrographs of PMMA submicrospheres before and after exposure to an electron beam (at 3 kV and 10 μA for 30 sec). (a) Obtained in an aqueous-acetone dispersion medium. Shrinkage is 7%. (b) Obtained in distilled water. The shrinkage is 18%.

All the samples despite the preparation conditions and particle size during electron microscopic investigation revealed approximately the same ability to self-assembly (Fig. 2). The absolute reflection spectra of the three-dimensional PhCs were obtained in a range of incident angles between 12° and 84°. The reflection spectrum at the angle of incidence of 56° revealed a remarkable feature wherein the main peak splits into two ones and both peaks show nearly equal reflectivity and linewidth. This phenomenon is called the multiple Bragg diffraction of light.

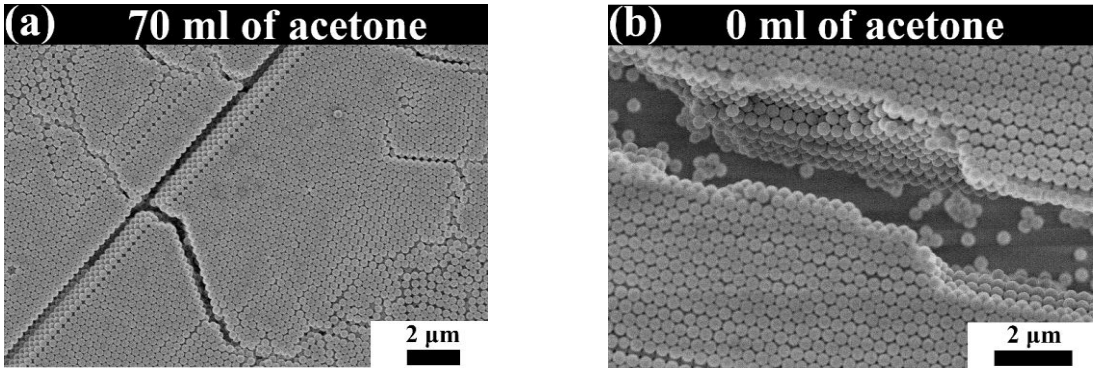

Figure 2. SEM images of photonic crystals based on artificial opals, obtained from PMMA submicron particles by a method of horizontal evaporation of the water-acetone dispersion medium (a) and distilled water (b).

According to the Bragg-Snell law [26], an estimating of the intensity of the maximum absolute reflectance in the direct fall was made using:

$$\lambda_{max}=d_{111}\sqrt{n_{eff}^2-\sin^2\theta}, \quad (1)$$

where d_{111} is the distance between (111) planes, θ is the angle of incidence, n_{eff} is the effective refractive index. Thus, the calculated absolute reflectance maximum at a normal incidence is 98% (Fig. 3b).

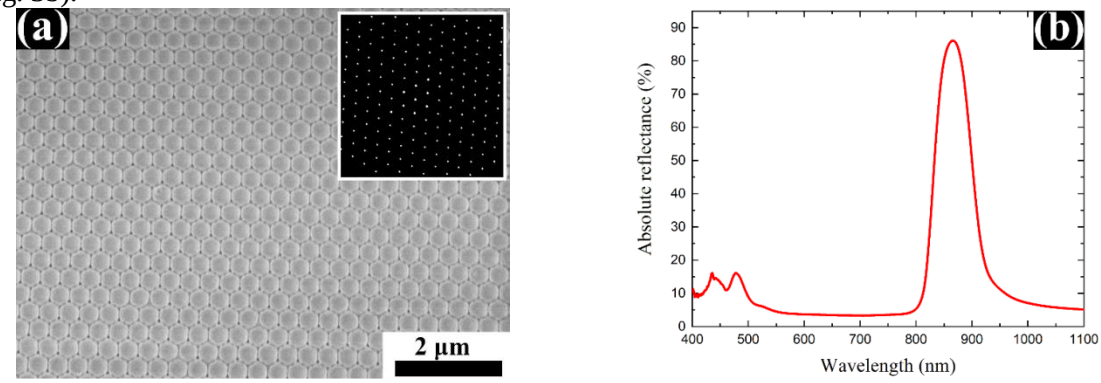

Figure 3. (a) SEM image of (111) surface of a three-dimensional photonic crystal obtained based on PMMA submicrospheres. The diameter of the beads is 367 nm. The inset demonstrates the Fourier transform and shows a single crystal structure. (b) An absolute reflectance spectrum of the (111) surface shown in Fig. 3a. The spectrum was obtained at the incident angle of 12°. The absolute reflectance is 87% at λ = 865 µm.

It is well known that the formation of ordered close-packed arrays requires the monodispersity and stability of the spherical particles, and the diameters should not vary by more than 5-8% [27] (Fig. 3a). However, in Fig. 2a, it is seen that small (about 5–10 µm) highly ordered domains are formed, alternating with regions (several micrometers) where the short-range order periodicity is observed. It is shown that surface tension plays one of the most important roles in self-assembly. Besides, it was experimentally established that the greater the order of opal film, the more defects in it. The greater the order, the deeper the cracks. This fact is especially noticeable for large particles that settle faster.

The three-dimensional photonic crystals based on the inverse opals from various precursors are obtained (Fig. 4).

4. Conclusion

To increase the morphological stability of the structure of the opal template, the PMMA submicrospheres were synthesized using the emulsion polymerization in the aqueous-acetone

dispersion medium. The SEM, ATR IR spectroscopy and DSC revealed the effect of the acetone content on the morphological features of the PMMA beads and the modification of mesoporous films, as well as their optical, physical, and chemical properties. It was shown that the degree of the shrinkage of the polymer submicrospheres B is higher compared to submicrospheres A and is 18–25% and 7–16%, respectively. It was found that the PMMA particles become stronger, harder, and more viscous with the addition of a certain amount of acetone. The complex dependencies of the particle shrinkage on various factors were experimentally discovered. These observed dependencies are of considerable interest and require additional research.

The ATR IR spectroscopy showed that the PMMA submicrospheres contain a significant amount of water, the evaporation of which leads to the shrinkage of the beads.

It was experimentally established that the optimal ratio of the chemicals to obtain a stable PhC of the PMMA.

The results of the study of the PMMA submicrospheres, as well as the opal structures obtained on their basis, can be useful in the fields of therapy and biological labeling, bio-detection and bio-imaging, manufacturing technologies for solar cells, temperature sensors and three-dimensional displays, multifunctional luminescence, battery electrolytes, and other nanotechnologies.

5. Acknowledgments

We are grateful to the Krasnoyarsk Regional Center of Research Equipment of Federal Research Center «Krasnoyarsk Science Center SB RAS» for the provided equipment. The authors are also grateful to the Russian Foundation for Basic Research for financial support (grant No. 18-42-243013).

6. References

[1] Ali U, Karim K J A and Buang N A 2015 *Polym. Rev.* **55** 678-705.
[2] Venditti I 2019 *King Saud Univ. - Sci.* **31** 398-411.
[3] Nyk M, Kumar R, Ohulchanskyy T Y, Bergey E J and Prasad P N 2008 *Nano Lett.* **8** 3834-3838.
[4] Chen Z, Fu M, Wu Z, Li C and Jiang J 2020 *Journal of Physics: Conference Series* **1622** 012066.
[5] Li J, Chen D and Chen G 2005 *Anal. Lett.* **38** 1127-1136.
[6] Lin S Y, Fleming J G, Hetherington D L, Smith B K, Biswas R, Ho K M, Sigalas M M, Zubrzycki W, Kurtz S R and Bur J 1998 *Nature* **394** 251-253.
[7] Glushko O, Brunner R, Meisels R, Kalchmair S and Strasser G 2012 *Opt. Express* **20** 17174.
[8] Wang H, Gu X, Hu R, Lam J W Y, Zhang D, Tang B Z, van de Lagemaat J, Frank A J, Li Y-P, Ma Y-G, Sun H-B, Zhang D, Wiersma D and Ozin G A 2016 *Chem. Sci.* **7** 5692-5698.
[9] Gu Z Z, Yu Y H, Zhang H, Chen H, Lu Z, Fujishima A and Sato O 2005 *Appl. Phys. A Mater. Sci. Process.* **81** 47-49.
[10] Waterhouse G I N, Chen W T, Chan A and Sun-Waterhouse D 2018 *ACS Omega* **3** 9658-9674.
[11] Wang Y, Dou S, Shang L, Zhang P, Yan X, Zhang K, Zhao J and Li Y 2018 *Crystals* **8** 453.
[12] Lee K T, Lytle J C, Ergang N S, Oh S M and Stein A 2005 *Adv. Funct. Mater.* **15** 547-556.
[13] Miklyaev Y V, Karpeev S V, Dyachenko P N, Pavelyev V S and Poletaev S D 2008 Fabrication of three-dimensional photonics crystals by interference lithography with low light absorption *Computer Optics* **32(4)** 357-360.
[14] Shetty P P, Zhang R, Angle J P, Braun P V and Krogstad J A 2018 *Chem. Mater.*
[15] Armstrong E, Khunsin W, Sotomayor Torres C M, Osiak M and O'Dwyer C 2014 *ECS Trans.* **58** 7-14.
[16] Kamitani K, Hyodo T, Shimizu Y and Egashira M 2010 *J. Mater. Sci.* **45** 3602-3609.
[17] D'Amato R, Venditti I, Russo M V and Falconieri M 2006 *J. Appl. Polym. Sci.* **102** 4493-4499.
[18] Nemtsev I V, Shabanova O V, Shestakov N P, Cherepakhin A V and Zyryanov V Y 2019 *Appl. Phys. A* **125** 738-750.
[19] De Angelis R, Venditti I, Fratoddi I, De Matteis F, Prosposito P, Cacciotti I, D'Amico L, Nanni

F, Yadav A, Casalboni M and Russo M V 2014 *J. Colloid Interface Sci.* **414** 24-32.
[20] Nemtsev I V, Shabanova O V and Shabanov A V 2012 *Sib. J. Sci. Technol.* **1** 126-129.
[21] Shabanova O V, Korshunov M A, Nemtsev I V and Shabanov A V 2016 *Nanotechnologies Russ.* **11** 633-639.
[22] Nemtsev I V, Tambasov I A, Ivanenko A A and Zyryanov V Y 2018 *Photonics Nanostructures Fundam. Appl.* **28** 37-44.
[23] Xia T, Luo W, Hu F, Qiu W, Zhang Z, Lin Y and Liu X Y 2017 *ACS Appl. Mater. Interfaces* **9** 22037-22041.
[24] Yoo J-H, Kwon H-J, Paeng D, Yeo J, Elhadj S and Grigoropoulos C P 2016 *Nanotechnology* **27** 145604.
[25] Huang Y, Zhou J, Su B, Shi L, Wang J, Chen S, Wang L, Zi J, Song Y and Jiang L 2012 *J. Am. Chem. Soc.* **134** 17053-17058.
[26] Wang J Q, Wu S, Ji X, Li J, Zhang R and Zhang M 2016 *Mater. Res. Express* **3** 045014.
[27] Stein A 2001 *Microporous Mesoporous Mater.* **44-45** 227-239.